

Repositioning Irsogladine to Hsp90 Inhibitor

Young Ho Seo*

College of Pharmacy, Keimyung University, Daegu 704-701, Korea. *E-mail: seoyho@kmu.ac.kr
Received January 14, 2015, Accepted March 4, 2015, Published online April 28, 2015

Heat shock protein 90 (Hsp90) is a ubiquitous adenosine triphosphate (ATP)-dependent molecular chaperone and represents an attractive cancer therapeutic target due to its role in maintaining the correct folding and stability of many oncogenic proteins. In our effort to repurpose existing drugs to Hsp90 inhibitors, we screened Food and Drug Administration (FDA) approved drugs based on chemical structure similarity and discovered that a mucosal protective drug, irsogladine, inhibits the Hsp90 folding machinery. *In vitro* fluorescence polarization assay and cell-based mechanism study demonstrate that irsogladine binds to the ATP-binding pocket in N-terminal domain of Hsp90 and impairs the Hsp90 chaperoning function. Consequently, irsogladine induces the downregulation of Hsp90 client proteins including Her2, Akt, and Cdk4 and upregulation of the co-chaperone Hsp70.

Keywords: Cancer, Computer modeling, Drug repositioning, Heat shock protein 90, Irsogladine

Introduction

Drug repositioning, also known as drug repurposing, is the process of finding new indications for existing drugs.^{1,2} Historically, drug repositioning has proved fruitful in bringing new therapies to the market. Successful examples of drug repositioning include the repositioning of thalidomide from an antiemetic to treat multiple myeloma, and sildenafil from angina to erectile dysfunction.² The strategy of drug repositioning offers a number of benefits in drug discovery, including lower drug development cost, reduction of research and development timeline for approval by up to 3–5 years, and, more importantly, the higher success rate of drug development. These advantages of the drug repositioning strategy are due to the fact that repositioning candidates would have often been through several stages of clinical development and therefore have known pharmacokinetic and safety profiles. Accordingly, drug repositioning can offer a better risk-versus-reward trade-off compared with other drug development strategies.

Heat shock protein 90 (Hsp90) is an abundant and ubiquitous adenosine triphosphate (ATP)-dependent molecular chaperone that is responsible for maintaining the correct folding and stability of its substrate proteins, referred to as “client” proteins. Hsp90 has been reported to have more than 200 client proteins that are involved in natural and acquired immunity, signal transduction, and protein trafficking.^{3,4} Many of its clients are notorious oncogenic proteins, including EGFR, VEGFR, Her2, and Bcr-Abl.⁵ It is known that cancer cells are more dependent on Hsp90's function than normal cells due to their genetic instability and oncogenic stressors in the hypoxic, acidotic, and nutrient-deprived environment. Therefore, Hsp90 is often overexpressed in a range of cancers, and high levels of Hsp90 results in poor prognosis of cancer patients.^{6–9} In this regard, Hsp90 has received significant attention and become an appealing therapeutic target for cancer.

The molecular structure of Hsp90 revealed that it has three subunits: an N-terminal domain, a middle domain, and C-terminal domain. The N-terminal domain of Hsp90 has an ATP-binding and hydrolyzing pocket with ATPase activity. The binding of ATP to Hsp90 allows client protein loading to Hsp90, and the energy released by ATP hydrolysis enables client protein folding.⁴ Hence, most of Hsp90 inhibitors have been discovered to target the ATP-binding pocket in the N-terminal domain of Hsp90, and the mechanism of the inhibitors involves the displacement of ATP in the N-terminal domain and the consequent blockage of Hsp90's ATPase activity.^{10–13} Currently, more than 10 drug candidates are in different stages of clinical trials (Figure 1).¹⁴ Despite these advances, none of Hsp90 inhibitors is clinically approved to date, and there still remains a need for the discovery of small molecules with improved pharmacokinetic and safety profiles.

Results and Discussion

Structural analysis of Hsp90 (PDB code: IBYQ) indicated that the ATP-binding pocket in the N-terminal domain of Hsp90 consisted of a hydrophilic region and a hydrophobic region (Figure 2).¹⁵ The hydrophilic region of the pocket consists of Asn51, Asp93, Thr184, and three water molecules. The binding pose of adenosine diphosphate (ADP) in the ATP-binding pocket of Hsp90 has revealed that the adenine base of ADP penetrates into the hydrophilic region of the pocket and makes water-bridged hydrogen-bonding interactions with the Asn51, Asp93, and Thr184 residues, which is a major contributor to the ADP binding to the pocket. The β -phosphate group of ADP sticks out of the ATP-binding pocket and exposes itself to the solvent molecules at the mouth of the pocket. The hydrophobic region of the ATP-binding pocket consists of the π -rich amino acid residues Phe138, Trp162, and Tyr139, forming a deep

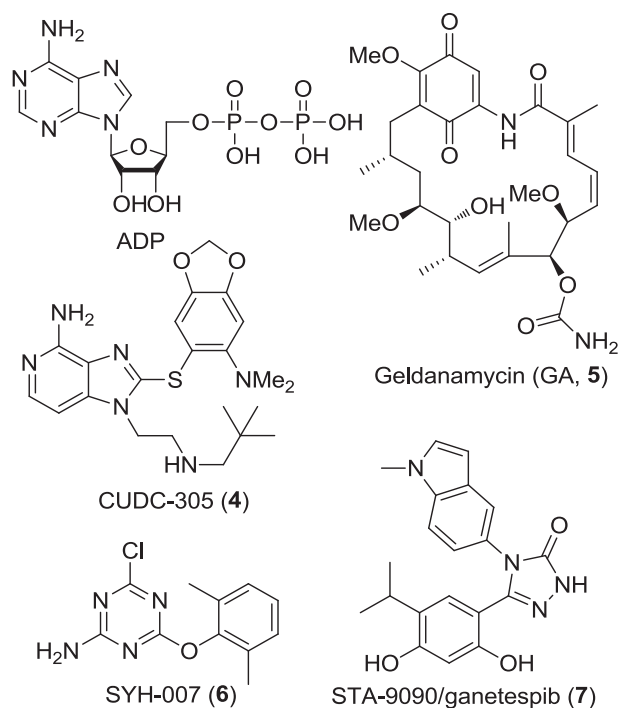


Figure 1. Structure of ADP and known Hsp90 inhibitors.

hydrophobic cavity. Unlike the hydrophilic region, ADP does not bind to hydrophobic region of the pocket.

To reposition existing drugs to Hsp90 inhibitors, we screened FDA-approved drugs based on chemical structure similarity and selected drugs having both a hydrophilic and a hydrophobic binding moiety, possibly fitting into the hydrophilic region and the hydrophobic region of ATP-binding pocket in the N-terminal domain of Hsp90.

The screening campaign provided us with three candidates: irsogladine (**1**), lamotrigine (**2**), and trimethoprim (**3**), as potential Hsp90 inhibitors (Figure 3). Irsogladine is a mucosal protective drug developed in Japan for the treatment of peptic ulcers and acute gastritis.¹⁶ Lamotrigine is an anticonvulsant drug used in the treatment of epilepsy and bipolar disorder, and trimethoprim is a bacteriostatic antibiotic used mainly in the prevention and treatment of urinary tract infections.^{17,18}

We first examined whether irsogladine (**1**), lamotrigine (**2**), and trimethoprim (**3**) could bind to Hsp90 using competition fluorescence polarization (FP) assay (Figure 4). In competition FP assay, a small molecule that is bound to the N-terminal ATP-binding pocket of Hsp90 will disrupt Fitc-labeled geldanamycin/Hsp90 complex, resulting in lowered millipolarization (mP) units. To assess the binding affinity of irsogladine (**1**), lamotrigine (**2**), and trimethoprim (**3**), Fitc-labeled geldanamycin was added to Hsp90 α in the presence of the test compounds (0.01, 0.1, 1, 30, 60, 100, 200, and 300 μ M) for 12 h, and the FP values in mP were measured. The FP assay demonstrated that irsogladine successfully bound to ATP-binding pocket in the N-terminal domain of human Hsp90 α , while lamotrigine and trimethoprim were not able to disrupt Fitc-labeled geldanamycin/Hsp90 complex. IC₅₀ values of

Results and Discussion

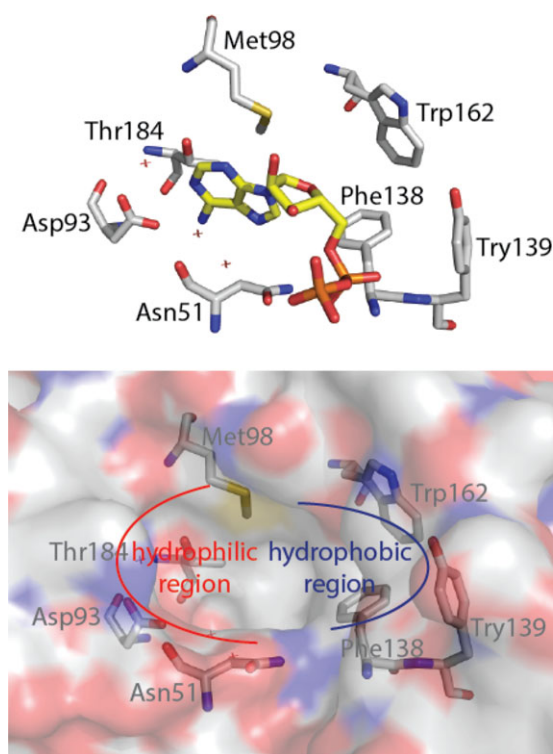


Figure 2. X-ray co-crystal structure of Hsp90 with ADP (PDB code: IBYQ) and apo-Hsp90. The carbon, oxygen, nitrogen, hydrogen, and phosphorus atoms of ADP are shown in yellow, red, blue, gray, and orange, respectively. Water molecules are highlighted in red asterisk symbols. The side chains of Hsp90's binding site are colored by the atom types (carbon, gray; oxygen, red; nitrogen, blue; sulfur, yellow) and labeled with their residue name.

irsogladine were determined using a nonlinear least-squares curve-fitting program, which provided the binding affinity of irsogladine as IC₅₀ = 14.8 μ M and K_i = 8.43 μ M.

Next we decided to investigate the cytotoxic effect of irsogladine on cancer cells. Accordingly, we assessed the cellular efficacy of irsogladine against H1975 cell line using colorimetric 3-(4,5-dimethylthiazol-2-yl)-5-(3-carboxymethoxyphenyl)-2-(4-sulfophenyl)-2H-tetrazolium (MTS) assay (Figure 5). H1975 is a gefitinib-resistant non-small-cell lung cancer cell (NSCLC) and its resistance is mediated by the mutation of T790M-EGFR and Met amplification.^{19,20} H1975 cells were incubated with varying concentrations of irsogladine (0.05, 0.1, 0.15, 0.2, 0.25, 0.3, 0.35, 0.4, 0.45, and 0.5 mM) for 72 h, and the viability of H1975 cells was measured. Interestingly, the result from the protein-based FP assay in Figure 4 did not translate to a similar potency in inhibiting the growth of NSCLC cells. Even though the cell viability slowly decreased in a concentration-dependent manner, irsogladine displayed a weak cellular cytotoxicity. This cytotoxicity is probably due to the fact that irsogladine was not able to effectively penetrate into the cytoplasm.

We next investigated the cellular biomarker of Hsp90 inhibition and evaluated the dose-dependent potency of

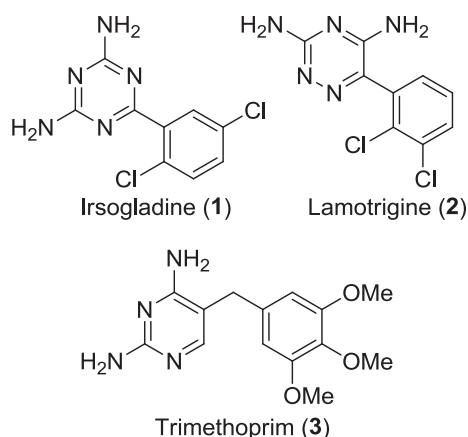


Figure 3. Structure of irsogladine, lamotrigine, and trimethoprim.

irsogladine for the downregulation of Hsp90 client proteins (Figure 6). H1975 cells were incubated with irsogladine (0, 10, 50, 100, 150, and 200 μM) for 48 h, and the expression of Hsp90 client proteins Her2, Akt, and Cdk4 along with Hsp70, Hsp90, and β -actin was measured by western blot, in which proteasomal degradation of Hsp90 client proteins and the transcriptional induction of Hsp70 are considered as cellular biomarkers of Hsp90 inhibition.²¹ As expected, irsogladine induced a significant degradation of Her2, Akt, and Cdk4 in a concentration-dependent manner. Her2 and Cdk4 began to degrade at 50 μM of irsogladine and were almost completely depleted at 150 μM . In contrast, the expression level of the co-chaperone Hsp70 was upregulated when exposed to irsogladine. Since β -actin was not dependent on the Hsp90 protein folding machinery, β -actin remained unchanged upon administration of irsogladine.

To investigate the binding pose of irsogladine in ATP-binding pocket of Hsp90, docking studies were performed using AutoDock4.2 (Figure 7). The crystal structure of Hsp90 (PDB code: 2XJX) was selected as the receptor model, and its native ligand AT13387 was removed. The molecular docking of irsogladine was carried out with the 3D coordinates of Hsp90. *In silico* modeling revealed that irsogladine fits the ATP-binding pocket in the *N*-terminal domain of Hsp90. 1,3,5-Triazine-2,4-diamine moiety was positioned in the hydrophilic region of the pocket, while 2,5-dichlorophenyl moiety was located in the hydrophobic cavity. The amino group at 2-position of 1,3,5-triazine formed water-bridged hydrogen-bonding interactions with Asn51 and Asp93, and the 2,5-dichlorophenyl ring of irsogladine formed proximal van der Waals interactions with the lipophilic amino acid residues Leu107, Val150, and Phe138. To confirm whether the amino groups at 2- and 4-positions of 1,3,5-triazine play a critical role in making hydrophilic interactions in ATP-binding pocket of Hsp90's *N*-terminal domain, we synthesized three *N*-methylated analogs of irsogladine to block the hydrogen-bonding interactions of the amino groups of 1,3,5-triazine, and measured their binding affinities (Scheme 1S and Figure 1S, Supporting information). As expected, the three

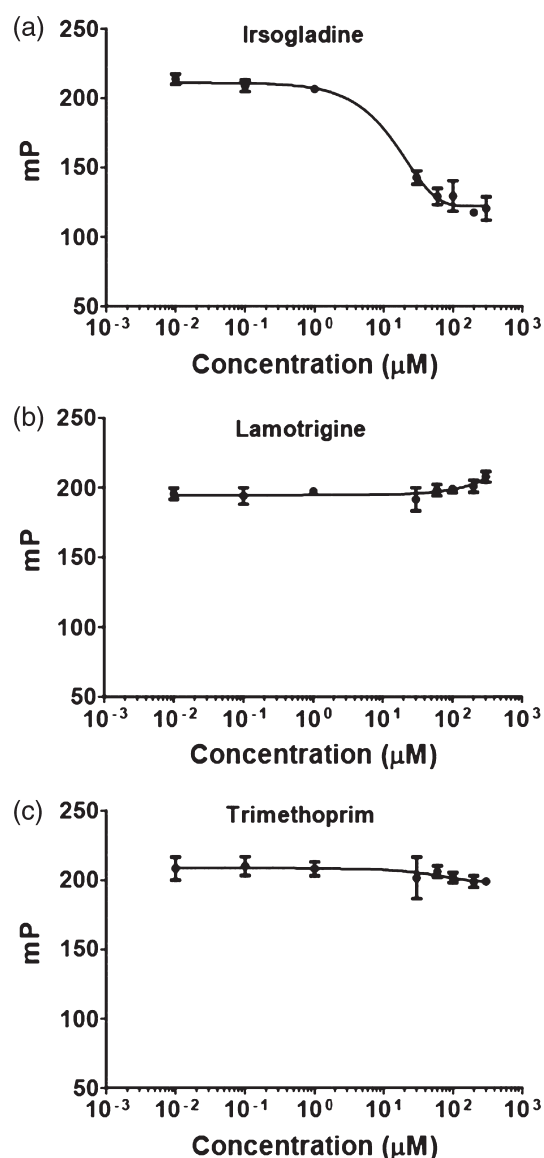


Figure 4. Inhibitory effect of irsogladine, lamotrigine, and trimethoprim against GM-FITC/Hsp90 α interactions. A mixture of 5 nM GM-FITC and 30 nM Hsp90 α was added, and the plate was incubated at 4 $^{\circ}\text{C}$. Data are the means \pm SD ($n = 3$). IC₅₀ values were calculated using the nonlinear least-squares curve-fitting program in Prism GraphPad software.

N-methylated analogs displayed significantly weak binding affinity compared to irsogladine, which indicated that the amino groups at 2- and 4-positions of 1,3,5-triazine participated in hydrogen-bonding interactions. Collectively, the docking study revealed that the hydrogen-bonding distance between the hydrogen atom at 2-amino group and the oxygen atom of Asp93 was 1.72 \AA , and the estimated binding energy (ΔG_b) and inhibition constants (K_i) of irsogladine using the Lamarckian genetic algorithm resulted in -7.59 kcal/mol and 2.74 μM , respectively. The K_i value obtained from *in silico* modeling was comparable to that from FP assay. Both K_i values from *in silico* modeling and *in vitro* FP assay were single-digit micromolar concentration.

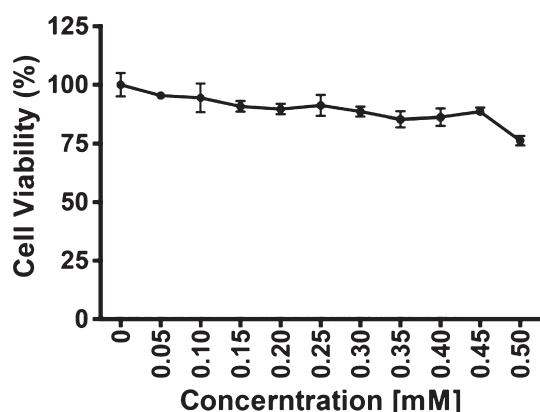


Figure 5. Effect of irsogladine on the cell proliferation of H1975. Cells were incubated with the indicated concentration of irsogladine for 72 h, and cell viability was measured by MTS assay. Data are presented as means \pm SD ($n = 4$).

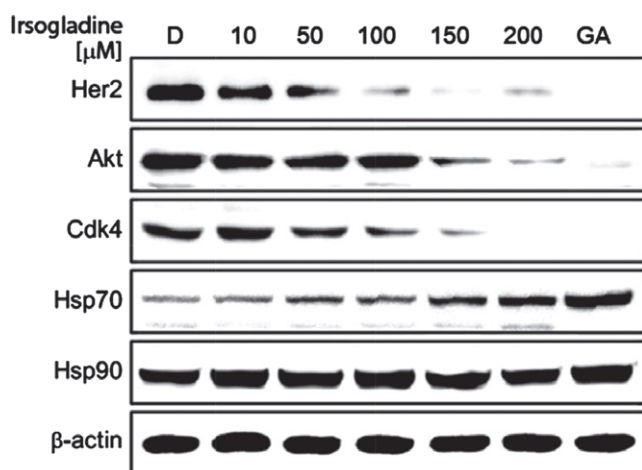


Figure 6. Effect of irsogladine on cellular biomarkers of Hsp90 inhibition. H1975 cells were incubated with the indicated concentration of irsogladine for 48 h, and the expression of Hsp90 client proteins (Her2, Akt, and Cdk4) along with Hsp70, Hsp90, and β -actin was analyzed by western blot. Geldanamycin (GA, 1 μ M) and DMSO (D) were employed as positive and a negative control, respectively.

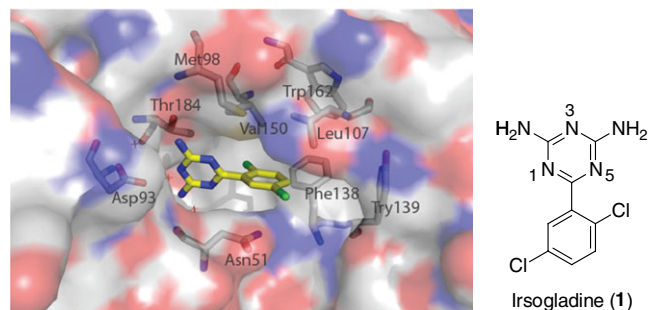


Figure 7. Molecular docking model of irsogladine with Hsp90 (PDB code: 2XJX). The carbon, oxygen, nitrogen, and chlorine atoms of irsogladine are illustrated in yellow, red, blue, and green, respectively. The side chains of binding site are colored by the atom types (carbon, gray; oxygen, red; nitrogen, blue) and labeled with their residue name.

Conclusion

In conclusion, we have discovered that irsogladine acts as an Hsp90 inhibitor and disrupts the Hsp90 folding machinery. *In vitro* FP assay and *in silico* modeling reveal that irsogladine binds the ATP-binding pocket in the *N*-terminal domain of Hsp90 with an IC_{50} value of 14.8 μ M. Consequently, irsogladine effects significant degradation of Hsp90's client proteins of Her2, akt, and Cdk4 and dose-dependent induction of the co-haperone Hsp70's expression level. These findings provide a valuable starting point of studying the structure–activity relationship (SAR) of irsogladine. Currently, our efforts are directed toward SAR optimization to improve the efficacy of irsogladine, and the result will be reported in due course.

Experimental

Materials. Antibodies specific for Her2, Akt, Cdk4, Hsp90, Hsp70, and β -actin were purchased from Cell Signaling Technology. Goat anti-rabbit IgG horseradish peroxidase conjugate was purchased from Santa Cruz Biotechnology. Cell Titer 96 Aqueous One Solution cell proliferation assay kit was purchased from Promega.

Fluorescence Polarization Assay. For competition studies, FP assays were performed as previously reported.²² Geldanamycin-FITC (GM-FITC), supplied by Enzo Life Sciences (Biomol International, Plymouth Meeting, PA, USA), was previously dissolved in DMSO to obtain 100 nM stock solutions and kept at -20°C until use. Hsp90 α was previously dissolved in the assay buffer (HFB) to form 2 μ M stock solutions and kept at -80°C until use. The compounds were previously dissolved in DMSO to obtain stock solutions and kept at -20°C . On the day of the experiment, the compounds were prepared by serial dilutions in the assay buffer (HFB) containing 20 mM HEPES, pH 7.3, 50 mM KCl, 5 mM MgCl_2 , 20 mM Na_2MoO_4 , and 0.01% NP40. Before each use, 0.1 mg/mL Bovine Gamma globulin and 2 mM DTT were freshly added. FP was performed in 96-well plates (Greiner Bio-One) using a plate reader (Infinite 200[®] Pro instrument Microplate Reader, TECAN, Männedorf, Switzerland). To evaluate the binding affinity of the molecules, GM-FITC solution (5 nM) was added to Hsp90 α (30 nM) in the presence of the test compounds at increasing concentrations (0.01, 0.1, 1, 30, 60, 100, 200, and 300 μ M) in a final volume of 100 μ L HFB buffer. For each assay, background wells (buffer only), tracer controls (free, fluorescent GM only), and bound GM controls (fluorescent GM in the presence of Hsp90 α) were included on each assay plate. The plate was mixed on a shaker at 4°C for 12 h, and the FP values (in mP) were measured at room temperature with an excitation wavelength of 495 nm and an emission wavelength at 530 nm. The IC_{50} values were calculated as the inhibitor concentration at which 50% of the tracer is displaced, and determined from a plot using nonlinear least-squares analysis. The K_i value was calculated from the IC_{50} value using the Cheng–Prusoff equation. Each data point was the average of

triplicate wells. All experimental data were analyzed using *Prism GraphPad* software.

Cell Culture. H1975 cells were grown in RPMI 1640 with L-glutamine supplemented with streptomycin (500 mg/mL), penicillin (100 units/mL), and 10% fetal bovine serum (FBS). Cells were grown to confluence in a humidified atmosphere (37 °C, 5% CO₂).

Effect of Irsogladine on Cell Proliferation. Cells were seeded at 3000 cells per well in a clear 96-well plate, the medium volume was brought to 100 µL, and the cells were allowed to attach overnight. The next day, varying concentrations of irsogladine or 1% DMSO vehicle control were added to the wells. Cells were then incubated at 37 °C for 24 h. Cell viability was determined using the Promega Cell Titer 96 Aqueous One Solution cell proliferation assay. After incubation with the compounds, 20 µL of the assay substrate solution was added to the wells, and the plate was incubated at 37 °C for an additional 1 h. Absorbance at 490 nm was then read on the Tecan Infinite F200 Pro plate reader (Tecan, Männedorf, Switzerland), and values were expressed as percentage absorbance from cells incubated in DMSO alone.

Western Blot. Cells were seeded in 60-mm culture dishes (5 × 10⁵/dish), and allowed to attach overnight. Irsogladine was added at the concentrations indicated in Figure 6, and the cells were incubated for an additional 48 h. For comparison, cells were also incubated with DMSO (1%) or geldanamycin (1 µM) for 24 h. Cells were harvested in ice-cold lysis buffer (23 mM Tris-HCl pH 7.6, 130 mM NaCl, 1% NP40, 1% sodium deoxycholate, 0.1% SDS), and 20 µg of lysate per lane was separated by SDS-PAGE and followed by transfer to a PVDF membrane (Bio-Rad, Hercules, CA, USA). The membrane was blocked with 5% skim milk in TBST, and then incubated with the corresponding antibody (Her2, Akt, Cdk4, Hsp90, Hsp70, or β-Actin). After binding of an appropriate secondary antibody coupled to horseradish peroxidase, proteins were visualized by electrochemical luminescence (ECL) according to the instructions of the manufacturer (Thermo Scientific, Waltham, MA, USA).

Docking Studies. *In silico* docking of irsogladine with the 3D coordinates of the X-ray crystal structures of the N-terminal domain of human Hsp90 (PDB code: 2XJX) was accomplished using the AutoDock program downloaded from the Molecular Graphics Laboratory of the Scripps Research Institute. The AutoDock program was chosen because it uses a genetic algorithm to generate the poses of the ligand inside a known or predicted binding site utilizing the Lamarckian version of the genetic algorithm, where the changes in conformations adopted by molecules after *in situ* optimization are used as subsequent poses for the offspring. In the docking experiments carried out, water was removed from the 3D X-ray coordinates, while Gasteiger charges were placed on the X-ray structures of the N-terminal domain of Hsp90 along with irsogladine using tools from the AutoDock suite. A grid box centered on the N-terminal Hsp90 domain with definitions

of 60_60_60 points and 0.375 Å spacing was chosen for ligand docking experiments. The docking parameters consisted of setting the population size to 150, the number of generations to 27 000, and the number of evaluations to 25 000 000, while the number of docking runs was set to 50 with a cutoff of 1 Å for the root-mean-square tolerance for the grouping of each docking run. The docking model of human Hsp90 with irsogladine is depicted in Figure 7, the rendering of which was done using PyMol (DeLano Scientific).

Supporting Information. Additional supporting information is available in the online version of this article.

References

1. G. Jin, S. T. Wong, *Drug Discov. Today* **2014**, *19*, 637.
2. T. T. Ashburn, K. B. Thor, *Nat. Rev. Drug Discov.* **2004**, *3*, 673.
3. V. C. da Silva, C. H. Ramos, *J. Proteomics* **2012**, *75*, 2790.
4. M. Taipale, D. F. Jarosz, S. Lindquist, *Nat. Rev. Mol. Cell Biol.* **2010**, *11*, 515.
5. D. Mahalingam, R. Swords, J. S. Carew, S. T. Nawrocki, K. Bhalla, F. J. Giles, *Br. J. Cancer* **2009**, *100*, 1523.
6. Q. Cheng, J. T. Chang, J. Geradts, L. M. Neckers, T. Haystead, N. L. Spector, H. K. Lyerly, *Breast Cancer Res.* **2012**, *14*, R62.
7. D. B. Solit, G. Chiosis, *Drug Discov. Today* **2008**, *13*, 38.
8. G. Chiosis, L. Neckers, *ACS Chem. Biol.* **2006**, *1*, 279.
9. L. Whitesell, S. L. Lindquist, *Nat. Rev. Cancer* **2005**, *5*, 761.
10. L. Whitesell, E. G. Mimnaugh, B. De Costa, C. E. Myers, L. M. Neckers, *Proc. Natl. Acad. Sci. USA.* **1994**, *91*, 8324.
11. T. Lee, Y. H. Seo, *Bioorg. Med. Chem. Lett.* **2013**, *23*, 6427.
12. Y. Wang, J. B. Trepel, L. M. Neckers, G. Giaccone, *Curr. Opin. Investig. Drugs* **2010**, *11*, 1466.
13. R. Bao, C. J. Lai, H. Qu, D. Wang, L. Yin, B. Zifcak, R. Atoyian, J. Wang, M. Samson, J. Forrester, S. DellaRocca, G. X. Xu, X. Tao, H. X. Zhai, X. Cai, C. Qian, *Clin. Cancer Res.* **2009**, *15*, 4046.
14. K. Jhaveri, T. Taldone, S. Modi, G. Chiosis, *Biochim. Biophys. Acta* **2012**, *1823*, 742.
15. W. M. Obermann, H. Sondermann, A. A. Russo, N. P. Pavletich, F. U. Hartl, *J. Cell Biol.* **1998**, *143*, 901.
16. F. Ueda, S. Aratani, K. Mimura, K. Kimura, A. Nomura, H. Enomoto, *Arzneimittelforschung* **1984**, *34*, 474.
17. A. F. Cohen, L. Ashby, D. Crowley, G. Land, A. W. Peck, A. A. Miller, *Br. J. Clin. Pharmacol.* **1985**, *20*, 619.
18. S. K. Sim, *Am. J. Pharm. Sci. Support Public Health* **1971**, *143*, 165.
19. J. G. Paez, P. A. Janne, J. C. Lee, S. Tracy, H. Greulich, S. Gabriel, P. Herman, F. J. Kaye, N. Lindeman, T. J. Boggon, K. Naoki, H. Sasaki, Y. Fujii, M. J. Eck, W. R. Sellers, B. E. Johnson, M. Meyerson, *Science* **2004**, *304*, 1497.
20. R. Sordella, D. W. Bell, D. A. Haber, J. Settleman, *Science* **2004**, *305*, 1163.
21. L. Wright, X. Barril, B. Dymock, L. Sheridan, A. Surgenor, M. Beswick, M. Drysdale, A. Collier, A. Massey, N. Davies, A. Fink, C. Fromont, W. Aherne, K. Boxall, S. Sharp, P. Workman, R. E. Hubbard, *Chem. Biol.* **2004**, *11*, 775.
22. J. Kim, S. Felts, L. Llauger, H. He, H. Huez, N. Rosen, G. Chiosis, *J. Biomol. Screen.* **2004**, *9*, 375.